NEURO-FUZZY CONTROL OF A DUAL STAR INDUCTION MACHINE

L. BENTOUHAMI R. ABDESSEMED Y. BENDJEDDOU E. MERABET
LEB-Research Laboratory Department of Electrical Engineering, University of Batna-2.
Street Chahid Mohamed El Hadi Boukhlouf, 05000. Batna, Algeria, l.bentouhami@univ-bba.dz.

Abstract: *This paper presents a new approach to the speed control of dual star induction machine (DSIM). The new technique uses a Neuro-Fuzzy Control (NFC) with an indirect field oriented method. For realize a control of this machine, two voltage source inverters of PWM techniques are introduced. Simulation results are presented for NFC controller, the results are compared with the results obtain from a Proportional Integral (PI) controller. It is observed that the NFC controller give better responses and robustness for the speed control of this machine with introduces load disturbances and parameters variations, such as an increased rotor resistance and moment of inertia.*

Key words: *Dual star induction machine (DSIM), Indirect field oriented control (IFOC), Voltage source inverter (VSI) and Neuro-fuzzy controller (NFC).*

1. Introduction

The inherent disadvantages of DC drives have prompted continual progress in the area of AC drives. Among AC drives, induction machine drives are widely used [1]. Multi-phase machines are AC machines characterized by a stator winding composed of generic number of phases. Actually, electric drive and generation technology multiphase machine has several advantages over the traditional three phase machine such as reducing the amplitude and increasing the frequency of torque pulsation, reducing the rotor harmonic current per phase without increasing the voltage per phase, lowering the dc-link current harmonics and higher reliability, high fault tolerance [2,3,4,5,6]. This characteristic makes them convenient in high power and/or high current applications, such as ship propulsion, aerospace applications, and electric/ hybrid vehicles (EV) [7], other suitable applications are pumps, fans, compressors, rolling mills, cement mills, mine hoists…[8]. A common type of multiphase machine is the dual star induction machine (DSIM). This machine has been used in many applications since the late 1920s [9]. The main difficulty in the asynchronous machine control resides in the fact that complex coupling exists between the field and the torque. The vector control assures decoupling between the field and the torque is made similar to that of a DC machine [10]. The indirect vector control scheme of the dual stator winding induction machine is based on the assumption that the machine can be treated as two independent induction machines coupled through the same rotor shaft [11,12].
Emil Levi [13] provides a review of the recent developments in the area of multiphase induction motor control. The conventional PI and PID controllers are employed in speed and current controller, but these controllers are very sensitive to machine parameters variation, load disturbances and along with step changes of command speed [14,15,16].

Numerous methods have been proposed to replace PI controller schemes, such as fuzzy logic controller (FLC) [17,18,19] and artificial neural networks (ANN's) [20,21,22]. A simple fuzzy controller implemented in the motor drive speed control has a narrow speed operation and needs much manual adjusting by trial and error if high performance is wanted [15]. On the other hand, it is extremely tough to create a serial of training data for ANN that can handle all the operating modes [23].

A Neuro-Fuzzy Controller, or simply NFC controller for the induction motor drive, which has the advantages of both FLC and ANN is proposed.

So, in this paper, a NFC for speed control of a DSIM drive system is proposed. Neuro-Fuzzy (NFC) developed in the early 90s by Jang [24,25,26], combines the concepts of fuzzy logic and neural networks to form a hybrid intelligent system that enhances the ability to automatically learn and adapt. An ANN is used to adjust input and output parameters of membership functions in FLC. The back propagation learning algorithm is used for training this network.

The DSIM is preliminary simulated with conventional PI speed regulator in order to establish a term of comparison. The results simulation obtained by using Matlab program is provided to confirm the validity of the proposed techniques.

The paper is organized as follows: the model of machine and IFOC description are given in section 2 and section 3 respectively. Section 4 is devoted to the design of the NFC controller. The simulation results are shown in section 5. The conclusions are given in section 6.

2. Machine Model

A common type of multiphase machine is the dual star induction machine (DSIM), where two sets of three-phase windings, spatially phase shifted by 30 electrical degrees, share a common stator magnetic core as shown in Fig.1 [17]. The modeling and control of DSIM in the original reference frame would be very difficult. For this reason, it is necessary to obtain a simplified model.

As consequence, also the mathematical modeling approach of DSIM is similar to the standard induction machine ones and usually it is obtained under the same simplifying assumptions [10] [17]:

- ❖ The two stars have same parameters,
- ❖ Motor windings are sinusoidally disturbed,
- ❖ The mutual leakage inductances are included,
- ❖ The magnetic saturation and the core losses are neglected.

The expressions for stator and rotor flux linkages are:

$$\emptyset_{ds1} = l_s i_{ds1} + L_m(i_{ds1} + i_{ds2} + i_{dr}) \quad (1)$$

$$\emptyset_{qs1} = l_s i_{qs1} + L_m(i_{qs1} + i_{qs2} + i_{qr}) \quad (2)$$

$$\emptyset_{ds2} = l_s i_{ds2} + L_m(i_{ds1} + i_{ds2} + i_{dr}) \quad (3)$$

$$\emptyset_{qs2} = l_s i_{qs2} + L_m(i_{qs1} + i_{qs2} + i_{qr}) \quad (4)$$

$$\emptyset_{dr} = l_r i_{dr} + L_m(i_{ds1} + i_{ds2} + i_{dr}) \quad (5)$$

$$\emptyset_{qr} = l_r i_{qr} + L_m(i_{qs1} + i_{qs2} + i_{qr}) \quad (6)$$

The following voltage equations are written for a DSIM in the synchronous reference frame [9]:

$$v_{ds1} = R_s i_{ds1} + p\emptyset_{ds1} - \omega_s \emptyset_{qs1} \quad (7)$$

$$v_{qs1} = R_s i_{qs1} + p\emptyset_{qs1} + \omega_s \emptyset_{ds1} \quad (8)$$

$$v_{ds2} = R_s i_{ds2} + p\emptyset_{ds2} - \omega_s \emptyset_{qs2} \quad (9)$$

$$v_{qs2} = R_s i_{qs2} + p\emptyset_{qs2} + \omega_s \emptyset_{ds2} \quad (10)$$

$$v_{dr} = R_r i_{dr} + p\emptyset_{dr} - (\omega_{s-}\omega_{r)}\emptyset_{qr} \quad (11)$$

$$v_{qr} = R_r i_{qr} + p\emptyset_{qr} + (\omega_{s-}\omega_{r)}\emptyset_{dr} \quad (12)$$

In the induction machines, rotor winding has a short-circuited hence

$v_{dr} = 0$ and $v_{qr} = 0$.

The mechanical equation is given by:

$$T_{em} = P\frac{L_m}{L_m+L_r}\left[\emptyset_{dr}(i_{qs1} + i_{qs2}) - \emptyset_{qr}(i_{qs1} + i_{qs2})\right] \quad (13)$$

$$\frac{J}{P}p\omega_r = T_{em} - T_L - \frac{K_f}{P}\omega_r \quad (14)$$

Where ω_s, ω_r speed of synchronous reference frame and rotor electrical angular;

l_s, l_r stator and rotor inductances;

L_m resultant magnetizing inductance;

P number of pole pairs;

J moment of inertia;

T_L load torque;

K_f total viscous friction coefficient.

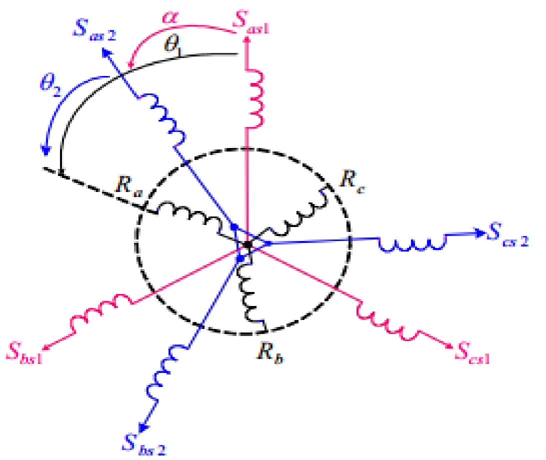

Fig. 1. Schematic of the dual star induction machine.

3. Indirect Field Oriented Control of a DSIM

The main goal of a field-oriented control (FOC) is to obtain decoupled control of electromagnetic torque and rotor flux of the motor as in DC machines [10][17]. The indirect field oriented control (IFOC) method is the most commonly used because of its relative simplicity and low cost of implementation.

The d-axis is aligned with the rotor flux space vector. In ideal field oriented control, the rotor flux linkage axis is forced to align with the *d*-axis, and it follows that: The direct flux equals to the reference:

$$\emptyset_{dr} = \emptyset_r^* \quad (15)$$

The quadratic component of the flux null:

$$p\emptyset_{dr} = \emptyset_{qr} = 0 \quad (16)$$

The commands/references voltage (v_{ds1}^*, v_{qs1}^*, v_{ds2}^* and v_{qs2}^*) are derived by substituting the (15) and (16) in (7)-(10) :

$$v_{ds1}^* = R_s i_{ds1} + l_s p i_{ds1} - \omega_s^*\left(l_s i_{qs1} + T_r \emptyset_r^* \omega_{sl}^*\right) \quad (17)$$

$$v_{qs1}^* = R_s i_{qs1} + l_s p i_{qs1} + \omega_s^*(l_s i_{ds1} + \emptyset_r^*) \quad (18)$$

$$v_{ds2}^* = R_s i_{ds2} + l_s p i_{ds2} - \omega_s^*(l_s i_{qs2} + T_r \emptyset_r^* \omega_{sl}^*) \quad (19)$$

$$v_{qs2}^* = R_s i_{qs2} + l_s p i_{qs2} + \omega_s^*(l_s i_{ds2} + \emptyset_r^*) \quad (20)$$

The component references of stator current and slip speed ω_{sl} can be expressed as

$$\omega_{sl}^* = \frac{R_r L_m}{(L_m+l_r)\emptyset_r^*} i_{qs}^* \quad (21)$$

$$i_{ds}^* = \frac{1}{L_m}\emptyset_r^* \quad (22)$$

$$i_{qs}^* = \frac{(L_m+l_r)}{P L_m \emptyset_r^*} T_{em}^* \quad (23)$$

Where: $i_{ds}^* = i_{ds1}^* + i_{ds2}^*$ (24)

$$i_{qs}^* = i_{qs1}^* + i_{qs2}^* \quad (25)$$

$$T_r = \frac{l_r}{R_r} \quad (26)$$

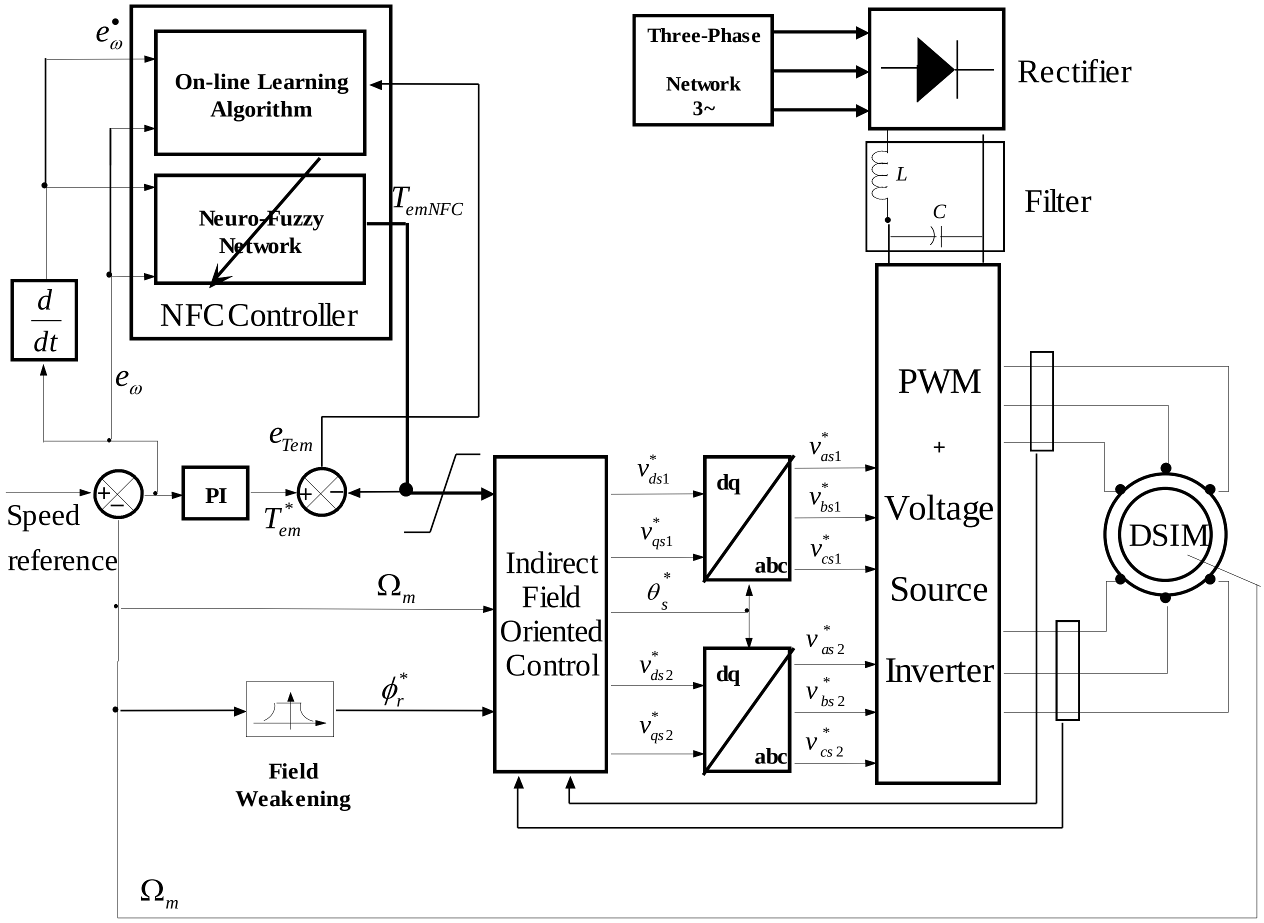

Fig. 2. Block diagram NFC with IFOC of regulation speed of DSIM.

he d-q-axes currents are relabeled as flux-producing (i_{ds}^*) and torque-producing (i_{qs}^*) components of the stator current phases, respectively.

T_r : denotes the rotor time constant.

For generate two sets of command/reference voltage vectors ($v_{ds1}^*, v_{qs1}^*, v_{ds2}^*$ and v_{qs2}^*), two independent pairs of PI controllers are introduced.

4. Design of the NFC controller

The proposed NFC incorporates fuzzy logic and a learning algorithm with a four-layer artificial neural network (ANN) structure as depicted in Fig. 2 with back propagation method. It describes the relationship between the speed error e_{ω}, its change $\dot{e}_{\omega}$ and the control signal T_{emNFC} [27]. The goal of the PI controller is to obtain a desired electromagnetic torque T_{em}^*.

e_{Tem} represents the error between the desired torque (T_{em}^*) and the control torque T_{em_NFC} (its current value give by NFC controller). The detailed discussions on different layers of the Neuro-fuzzy network fig. 3, are given below.

Layer I: Each input node in this layer corresponds to the specific input variable, the inputs of this layer are given by: $net_1^I = e_{\omega}$ and $net_2^I = \dot{e}_{\omega}$.

The outputs of this layer are given by

$y_1^I = f_1^I(net_1^I) = e_{\omega}$ and $y_2^I = f_2^I(net_2^I) = \dot{e}_{\omega}$

The weights of this layer are unity and fixed.

Layer II: Seven membership function based fuzzy set is utilized to obtain the fuzzy number for each input. In the propose NFC, Gaussian functions are chosen as the membership function as shown in fig. 4.

$$net_{1,j}^{II} = -\left(\frac{x_{1,j}^{II} - m_{1,j}^{II}}{\sigma_{1,j}^{II}}\right)^2 \tag{27}$$

$$net_{2,k}^{II} = -\left(\frac{x_{2,k}^{II} - m_{2,k}^{II}}{\sigma_{2,k}^{II}}\right)^2 \tag{28}$$

$$y_{1,j}^{II} = f_{1,j}^{II}\left(net_{1,j}^{II}\right) = exp\left(net_{1,j}^{II}\right) \tag{29}$$

$$y_{2,k}^{II} = f_{2,k}^{II}\left(net_{2,k}^{II}\right) = exp\left(net_{2,k}^{II}\right) \tag{30}$$

Where: $m_{1,j}^{II}$, $m_{2,k}^{II}$ and $\sigma_{1,j}^{II}$, $\sigma_{2,k}^{II}$ are the mean and the deviation of the Gaussian function.

Layer III: Every node in this layer is a fixed node labeled Π, for represent a rule base used in the FLC, a product operator is used in each node.

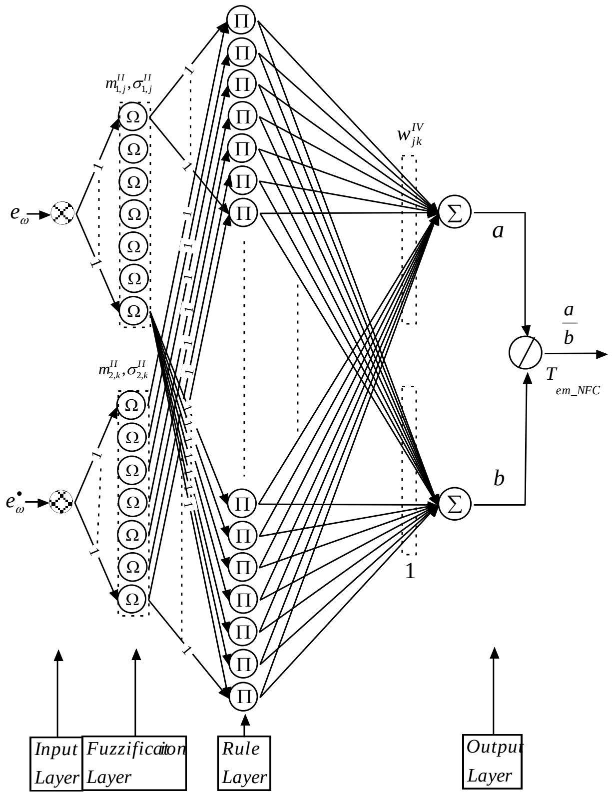

Fig. 3. Neuro-fuzzy network structure.

A 49 rules base for the NFC is given in Tab. 1.

$$net_{jk}^{III} = \left(x_{1,j}^{III} \times x_{2,k}^{III}\right), y_{jk}^{III} = f_{jk}^{III}\left(net_{jk}^{III}\right) = net_{jk}^{III} \tag{31}$$

The values of weights between layer III and layer II are unity.

Layer IV: The center of gravity method is used to determine the output of NFC. Each node equation is specified as

$$a = \sum_j \sum_k \left(w_{jk}^{IV} y_{jk}^{III}\right), \ \ \sum_j \sum_k y_{jk}^{III} \tag{32}$$

$$net_0^{IV} = \frac{a}{b}, y_0^{IV} = f_0^{IV}\left(y_0^{IV}\right) = \frac{a}{b} \tag{33}$$

w_{jk}^{IV} represent the values of the output membership functions used in the FLC as shown in fig. 5. y_0^{IV} is output of the layer IV. a and b are the numerator and the denominator of the function used in the center of area method, respectively. In the NFC, the goal of learning algorithm is adjustment the weightsw_{jk}^{IV}, the $m_{1,j}^{II}$, $m_{2,k}^{II}$ and $\sigma_{1,j}^{II}$, $\sigma_{2,k}^{II}$. For the learning algorithm we use the supervised gradient descent method. The error E we take for describe the back propagation algorithm.

$$E(l) = \frac{1}{2} e_{Tem}^2 \tag{34}$$

Where the error value can be written as

$$e_{Tem} = d - y \tag{35}$$

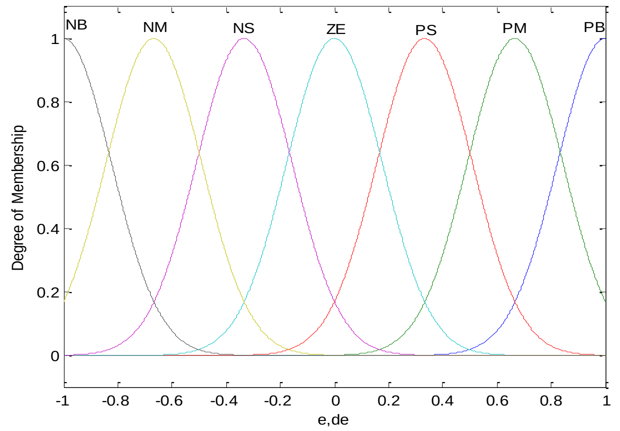

Fig. 4. Membership functions for inputs “e” and “de”.

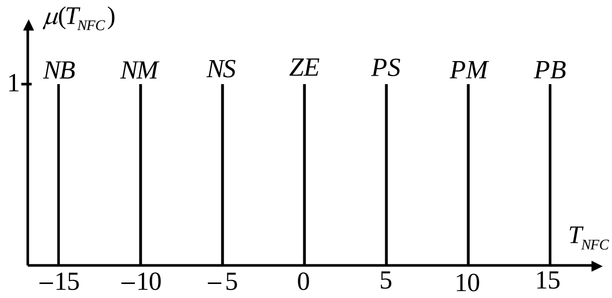

Fig. 5. Membership functions for output “T_{emNFC}”.

Table 1
Rules base for NFC control.

e/de	NB	NM	NS	ZE	PS	PM	PB
NB	NB	NB	NB	NB	NM	NS	ZE
NM	NB	NB	NB	NM	NS	ZE	PS
NS	NB	NB	NM	NS	ZE	PS	PM
ZE	NB	NM	NS	ZE	PS	PM	PB
PS	NM	NS	ZE	PS	PM	PB	PB
PM	NS	ZE	PS	PM	PB	PB	PB
PB	ZE	PS	PM	PB	PB	PB	PB

Where d is the desired torque control T_{em}^* (The output of PI controller) and y is the actual output (y is equal to the output of NFC “T_{emNFC}”).

4.1. The back propagation algorithm

Layer IV: The error expression for the input of this layer $\delta_0^{IV} = -\frac{\partial E}{\partial t_0^{IV}} = -\frac{\partial E}{\partial e}\frac{\partial e}{\partial y}\frac{\partial y}{\partial t_0^{IV}} = e$ (36)

The variations Δw_{jk}^{IV} of the weights w_{jk}^{IV} to minimize the error can be determined by the generalized delta rule as follows

$$\Delta w_{jk}^{IV} = -\frac{\partial E}{\partial w_{jk}^{IV}} = -\left[\frac{\partial E}{\partial t_0^{IV}}\right]\frac{\partial t_0^{IV}}{\partial a}\frac{\partial a}{\partial w_{jk}^{IV}} = \frac{1}{b}\delta_0^{IV} y_{jk}^{III} \tag{37}$$

Finally, the weights w_{jk}^{IV} can be updated to minimize the error as follows

$$w_{jk}^{IV}(t) = w_{jk}^{IV}(t-1) + \mu_w \Delta w_{jk}^{IV}(t) \tag{38}$$

Where μ_w is learning rate for w_{jk}^{IV}.

Layer III: The error received by this layer from layer IV is computed as

$$\delta_{jk}^{III} = -\frac{\partial E}{\partial t_{jk}^{III}} = \left[-\frac{\partial E}{\partial t_0^{IV}}\right]\frac{\partial t_0^{IV}}{\partial y_{jk}^{III}}\frac{\partial y_{jk}^{III}}{\partial t_{jk}^{III}} = \frac{1}{b}\delta_0^{IV}(w_{jk}^{IV} - y) \quad (39)$$

Layer II: The error received from Layer III is computed as

$$\delta_{1,j}^{II} = -\frac{\partial E}{\partial t_{1,j}^{II}} = \sum_k \left[\left(-\frac{\partial E}{\partial t_{jk}^{III}}\right)\frac{\partial t_{jk}^{III}}{\partial y_{1,j}^{II}}\frac{\partial y_{1,j}^{II}}{\partial t_{1,j}^{II}}\right] = \sum_k \delta_{jk}^{III} y_{jk}^{III} \quad (40)$$

$$\delta_{2,k}^{II} = -\frac{\partial E}{\partial t_{2,k}^{II}} = \sum_j \left[\left(-\frac{\partial E}{\partial t_{jk}^{III}}\right)\frac{\partial t_{jk}^{III}}{\partial y_{2,k}^{II}}\frac{\partial y_{2,k}^{II}}{\partial t_{2,k}^{II}}\right] = \sum_j \delta_{jk}^{III} y_{jk}^{III} \quad (41)$$

In this layer, the changes of $m_{1,j}^{II}$, $m_{2,k}^{II}$ and $\sigma_{1,j}^{II}$, $\sigma_{2,k}^{II}$ are written as

$$\Delta m_{1,j}^{II} = -\frac{\partial E}{\partial m_{1,j}^{II}} = \left[-\frac{\partial E}{\partial t_{1,j}^{II}}\right]\frac{\partial t_{1,j}^{II}}{\partial m_{1,j}^{II}} = \delta_{1,j}^{II}\frac{2\left(x_{1,j}^{II} - m_{1,j}^{II}\right)}{\left(\sigma_{1,j}^{II}\right)^2} \quad (42)$$

$$\Delta m_{2,k}^{II} = -\frac{\partial E}{\partial m_{2,k}^{II}} = \left[-\frac{\partial E}{\partial t_{2,k}^{II}}\right]\frac{\partial t_{2,k}^{II}}{\partial m_{2,k}^{II}} = \delta_{2,k}^{II}\frac{2(x_{2,k}^{II} - m_{2,k}^{II})}{(\sigma_{2,k}^{II})^2} \quad (43)$$

$$\Delta \sigma_{1,j}^{II} = -\frac{\partial E}{\partial \sigma_{1,j}^{II}} = \left[-\frac{\partial E}{\partial t_{1,j}^{II}}\right]\frac{\partial t_{1,j}^{II}}{\partial \sigma_{1,j}^{II}} = \delta_{1,j}^{II}\frac{2\left(x_{1,j}^{II} - m_{1,j}^{II}\right)^2}{\left(\sigma_{1,j}^{II}\right)^3} \quad (44)$$

$$\Delta \sigma_{2,k}^{II} = -\frac{\partial E}{\partial \sigma_{2,k}^{II}} = \left[-\frac{\partial E}{\partial t_{2,k}^{II}}\right]\frac{\partial t_{2,k}^{II}}{\partial \sigma_{2,k}^{II}} = \delta_{2,k}^{II}\frac{2(x_{2,k}^{II} - m_{2,k}^{II})^2}{(\sigma_{2,k}^{II})^3} \quad (45)$$

Membership parameters adaptation is obtained through the following:

$$m_{1,j}^{II}(t) = m_{1,j}^{II}(t-1) + \mu_m \Delta m_{1,j}^{II}(t) \quad (46)$$

$$m_{2,k}^{II}(t) = m_{2,k}^{II}(t-1) + \mu_m \Delta m_{2,k}^{II}(t) \quad (47)$$

$$\sigma_{1,j}^{II}(t) = \sigma_{1,j}^{II}(t-1) + \mu_\sigma \Delta \sigma_{1,j}^{II}(t) \quad (48)$$

$$\sigma_{2,k}^{II}(t) = \sigma_{2,k}^{II}(t-1) + \mu_\sigma \Delta \sigma_{2,k}^{II}(t) \quad (49)$$

Where μ_m and μ_σ are learning rates, respectively, for $m_{1(2),j(k)}^{II}$ and $\sigma_{1(2),j(k)}^{II}$.

4. Simulation results under proposed structure

Simulations results for FLC of DSIM based on IFOC are presented as follows:

The Fig. 6 presents the responses with the application of a rotor speed inversion with an increased moment of inertia (ΔJ % = +50%) on no load.

In Fig.7, the system is simulated for a step reference speed, with an increased rotor resistance (ΔRr% = +50%) followed by applying load torque (14N.m). The figure (8) presents responses to many reference speeds for an increased rotor resistance (ΔRr% = +50%) after t = 1.5s on no load.

Table 2 shows the parameters of the DSIM used for simulation whose general specifications are 4.5kW, 2753rpm, 220/380V, 2 poles.

Table 2
Motor parameters

Stator resistance	R_s=3.72 Ω
Rotor resistance	R_r=2.12 Ω
Stator leakage inductance	L_s=0.022 H
Rotor leakage inductance	L_r=0.006 H
Resultant magnetizing inductance	L_m=0.3672 H
Moment of inertia	J=0.0662 kg.m^2
Viscous friction coefficient	K_f=0.001kg.m^2/s

Fig. 6, shows the reference and simulated values of rotor speed, electromagnetic torque, direct and quadratic rotor flux respectively.

It can be seen in Fig. 6(a), that the rotor speed follows its reference (2500rpm) in a good manner when the load torque is zero, the PI controller for the rotor speed has the fast response time in transient state. The actual speed tracks the negative reference speed (-2500 rpm) for both controllers, after 2.5s the inertia variation ($J=1.5J_n$) increases the inversion time of rotating direction. The starting electromagnetic torque reaches until (66N.m) with PI and (62N.m) for NFC controllers, Fig. 6(b). This figure shows also that the electromagnetic torque decreases to stabilize

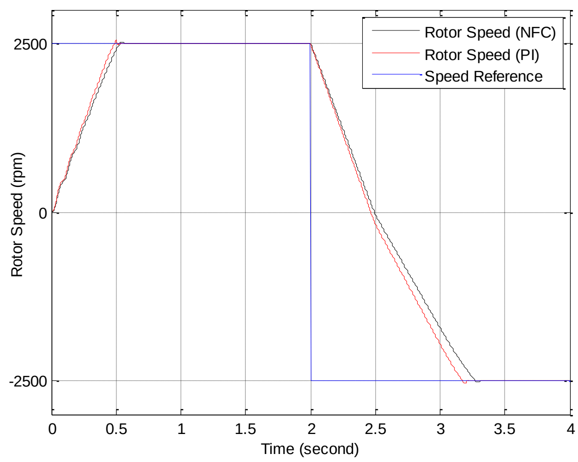

a) The rotor speed with PI and NFC Controllers.

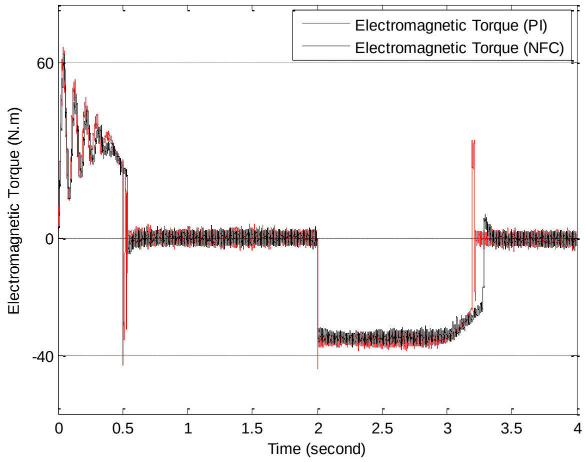

b) Electromagnetic torque response of PI and NFC controllers.

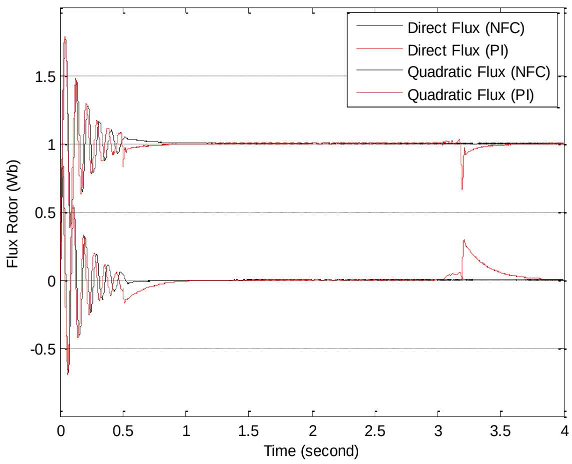

c) Direct and quadratic rotor flux.

Fig. 6. Simulated responses to inverse of the rotor speed at t = 2s with an increased moment of inertia (ΔJ % = +50%) at t = 2.5s with no load.

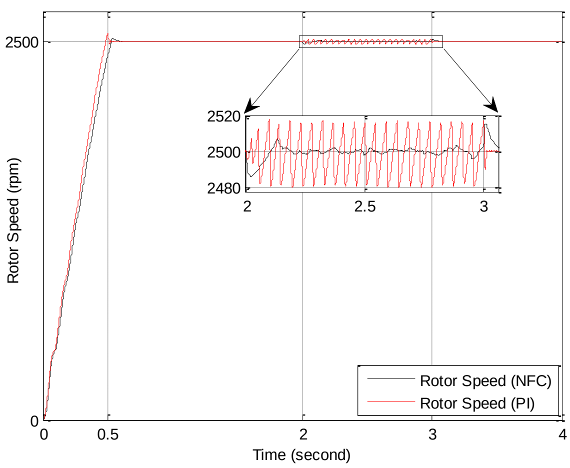

a) The rotor speed with PI and NFC Controllers.

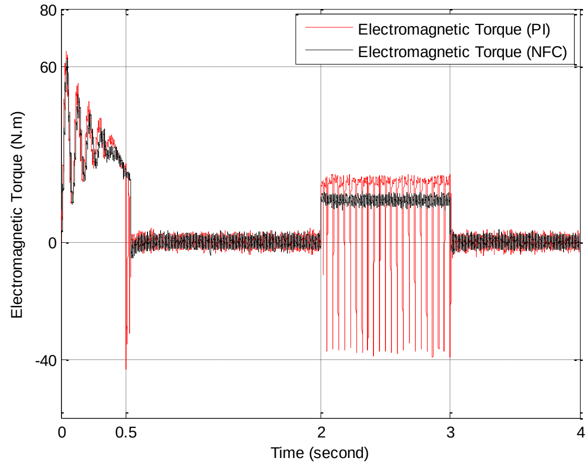

b) Electromagnetic torque response of PI and NFC controllers.

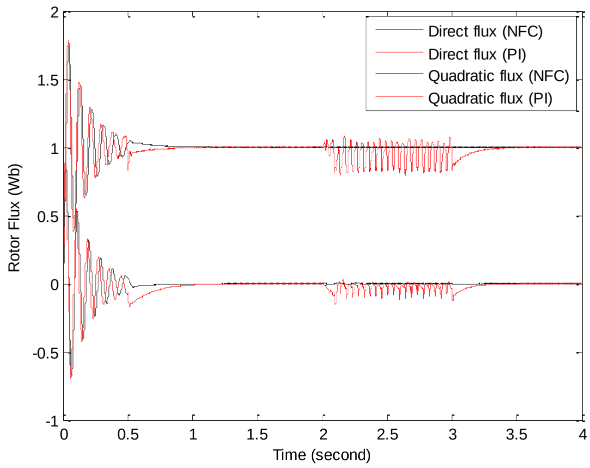

c) Direct and quadratic rotor flux.

Fig. 7. Simulated responses to a step reference speed, with an increased rotor resistance ($\Delta Rr\%$ = +50%) followed by applying load torque (14N.m).

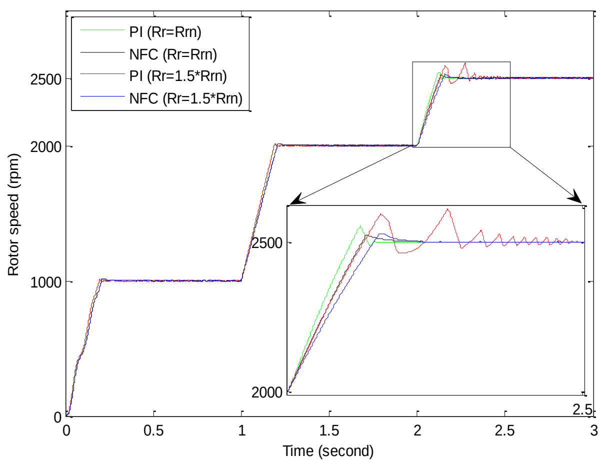

a) The rotor speed with PI and NFC Controllers.

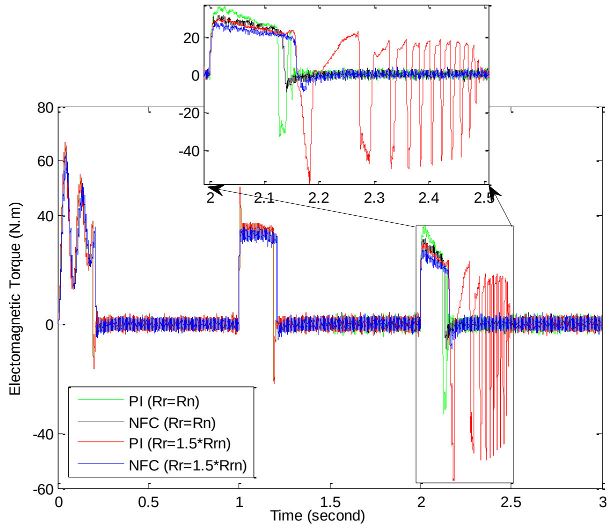

b) Electromagnetic torque response of PI and NFC controllers.

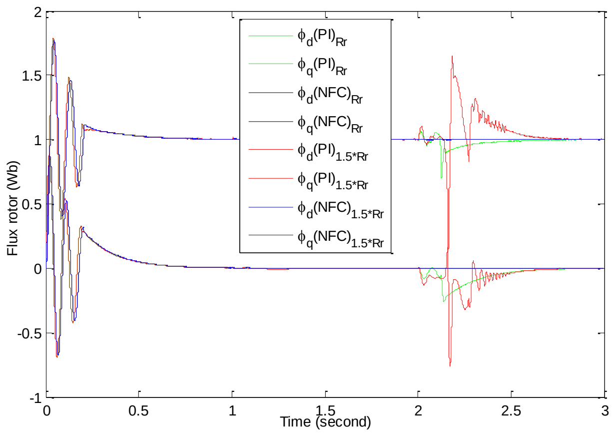

c) Direct and quadratic rotor flux.

Fig. 8. Simulated responses for a stairs reference speed (1000, 2000 and 2500 rpm) with different values of rotor resistance.

at a value of (-35N.m) for both controllers (second transient response) for forcing the rotor speed to follow the desired reference trajectory.

The rotor flux (direct and quadratic) are converge to the reference values in a short time, but important oscillations with PI controller are observed, Fig.6(c). Also, the NFC gives better performances compared to PI obtained in the case of inversing reference speed from 2500 rpm to -2500 rpm when the moment of inertia is varied.

The application of load torque (14N.m) at t=2s and it's elimination at t=3s, Fig. 7, when the rotor resistance changed ($Rr = 1.5Rr_n$) at t=1s, we see clearly that the NFC is insensitive to constant time variation contrary to the PI controller. Also, the applying of load torque leads speed oscillations in the case of this last, Fig. 7(a). These oscillations due to the electromagnetic torque harmonics. In Fig. 7(b), we see the same phenomenon for the rotor flux. When applying a load torque with PI controller, the direct flux oscillates between 1.05 and 0.8Wb, while the quadratic flux reaches -0.15Wb, Fig. 7(c).We see that the FLC gives the same performances when the load torque not varied.

The performances of the proposed NFC controller has been also tested for many reference speeds (1000, 2000 and 2500rpm) with different values of the rotor resistance, Fig. 8.

In Fig. 8(a), the rotor speeds reach their references (1000, 2000 and 2500 rpm), but they have important oscillations in the case of PI controller especially for 2500 rpm mostly with $Rr = 1.5Rr_n$. The same thing is observed for the electromagnetic torque when this latter oscillates until +22 and -57N.m with $Rr = 1.5Rr_n$ and 2500 rpm, Fig. 8(b). Also, Fig. 8(c) shows the same situation for the direct and quadratic rotor flux.

This comparison shows clearly that the NFC controller gives better performances and robustness than the PI controller.

5. Conclusion

In this paper, a new approach NFC control is established where four layer NN are used to adjust input and output parameters of membership functions in NFC. The simulation results show that the NFC give better performances compared to a traditional controller PI.

Also, the robustness tests show too that the NFC controller is more robust than the PI controller when load disturbances occurred, and when some motor parameters (i.e. rotor resistance and moment of inertia) were increased.

6. References

1. Yong-le Ai, Kamper M. J. and Le Roux A. D.: *Novel direct field and direct torque control of six-phase induction machine with special phase current waveform*. In: IEEE. Ind. App. Conf, 41st IAS(2006), vol. 2, pp. 805–812, 2006.
2. E. A. Klingshirn.: *High phase order induction motors – Part I: experimental results*. In: IEEE Trans. Power Applications.
3. Singh G.K..: *Multi-phase induction machine drive research – a survey*. In: Electr. Power Syst. Res., 2002, 61, pp. 139– 147, 2002.
4. Emil Levi.: *Multiphase Electric Machines for Variable-Speed Applications*. In: IEEE transactions industrial electronics, vol. 55, no. 5, may 2008.
5. V. Pant, G.K. Singh, S.N. Singh.: *Modeling of a multiphase induction machine under fault condition.* In: Proceedings IEEE The Third International Conference on Power Electronics and Drive Systems, PEDS'99, Hong Kong, July 26– 29, 1999, Vol. 1, pp.

92–97.
6. D. Hadiouche, H. Razik, and A. Rezzoug.: *On the Modeling and Design of Dual Stator Windings to Minimize Circulating Harmonic Currents for VSI Fed AC Machines*. In: IEEE Transactions On Industry Applications, Vol. 40, No. 2, pp. 506-515, March /April 2004.
7. K. Gopalkumar, Mahopatra.: *A novel scheme for six phase induction motor with open end windings.* In: 28th Annual Conference of IEEE Industrial Electronics Society, Spain. 5th-8th November, 2002.
8. Y. Zhao, T. A. Lipo.: *Space Vector PWM Control of Dual Three Phase Induction Machine Using Vector Space Decomposition*. In: IEEE Trans. Ind. Appl., Vol. 31, No. 5, pp. 1100-1109, September/October 1995.
9. P. L. Alger, E. H. Freiburghouse., and D. D. Chase.: *Double windings for turbine alternators*. In: AIEE Trans., vol. 49, pp. 226–244, Jan. 1930.
10. E. Merabet, R. Abdessemed, H. Amimeur and F. Hamoudi.: *Field-oriented Control of a Dual Star Induction Machine Using Fuzzy Regulators*. In: CIP, Sétif, Algérie, 2007.
11. A. R. Munoz and T. A. Lipo.: *Complex vector model of the squirrel cage induction machine including instantaneous rotor bar currents*. In: IEEE Transactions on Industry Applications, vol. 35, no. 6, pp. 1332-1340, Nov./Dec. 1999.
12. Z. Wu and 0. Ojo.: *Coupled circuit model simulation and air gap field calculation of a dual stator winding induction machine*. IEE Proceedings: Electric Power Applications, Vol. 153, Issue 3, pp. 387 -400, May 2006.
13. Emil Levi.: *Recent Developments in High Performance Variable-Speed Multiphase Induction Motor Drives*. In: Sixth International Symposium Nikola Tesla, Belgrade, Serbia. 18th–20th October, 2006.
14. Yi S. Y. and Chung M. J.: *Robustness of fuzzy logic control for an uncertain dynamic system.* In: IEEE Trans. Fuzzy Syst. vol. 6, pp. 216–224, May. 1998.
15. Uddin M. N., Radwan T. S. and Rahman M. A.: *Performances of fuzzy-logic-based indirect vector control for induction motor drive*. In: IEEE Trans. Ind. App., vol. 38, no. 5, pp. 1219–1225, Sep/Oct. 2002.
16. Krishnan R., Doran F.: *Study of parameter sensitivity in high performance inverter fed induction motor drive systems*. In: IEEE Trans. Ind. Appl., vol. 23, pp. 623635, Jul/Aug. 1987.
17. Radhwane Sadouni, Abdelkader Meroufel.: *Indirect Rotor Field-oriented Control (IRFOC) of a Dual Star Induction Machine (DSIM) Using a Fuzzy Controller*. In: Acta Polytechnica Hungarica., Vol. 9, No. 4, 2012.
18. Salima Lekhchine, Tahar Bahib, Youcef Soufi.: *Indirect rotor field oriented control based on fuzzy logic controlled double star induction machine*. In: Electrical Power and Energy Systems 57, pp. 206–211. 2014.
19. Elkheir Merabet, Hocine Amimeur, Farid Hamoudi and Rachid Abdessemed.: *Self–Tuning Fuzzy Logic Controller for a Dual Star Induction Machine*. In: Journal of Electrical Engineering & Technology Vol. 6, No. 1, pp. 133-138, 2011.
20. Meliani Bouziane, Meroufel Abdelkader.: *A Neural Network Based Speed Control of a Dual Star Induction Motor*. In: IJECE., Vol. 4, No. 6, December , pp. 952~961. 2014.
21. U. Michael, T. Wishart, and Ronald G. Harley.: *Identification and Control of Induction Machines Using: Artificial Neural Networks*. In: IEEE Transactions on Industry Applications, Vol. 31, no. 3, may/june 1995.
22. Salima Lekhchine, Tahar Bahi, Youcef Soufi, Hichem Merabet.: *Neural Fuzzy Speed Control For Six Phase Induction Machines*. In: International conference of control, engineering & information technology (CEIT'13), Vol.3, pp. 123-127, 2013.
23. M. N. Uddin, M. A. Abido, and M. A. Rahman.: *Development and implementation of a hybrid intelligent controller for interior permanent magnet synchronous motor drive*. In: IEEE Trans. Ind. Appl., vol. 40, no. 1, pp. 68–76, Jan./Feb. 2004.
24. J-S. R. Jang.: *ANFIS: Adaptive-Network-Based Fuzzy Inference Systems*. In: IEEE Trans. System, Man, and Cybernetics, vol. 23, no. 3, May/June, pp. 665-684. 1993.
25. J-S. R. Jang.: *Self-Learning Fuzzy Controllers Based on Temporal Back Propagation*. In: IEEE Trans. on Neural Networks, vol. 3, no. 5, pp. 714-723, Sept. 1992,
26. J-S. R. Jang, C-T. Sun.: *Neuro-Fuzzy Modeling and Control*. In: Proceedings of the IEEE, vol. 83, no. 3, pp.378-406, March 1995.
27. C. Elmas, O. Ustun, Hasan H. Sayan.: *A neuro-fuzzy controller for speed control of a permanent magnet synchronous motor drive*. In: Expert Systems with Applications 34 (2008) 657–664, 2008.